Detektorkonzepte der Hochenergie Astrophysik

Inhalt

- Motivation
- Kosmische Strahlung
- Direkte Beobachtung
  - Chandra, ACE und PAMELA
- Indirekte Beobachtung
  - Teilchenschauer in der Luft
  - Detektoren
    - Teilchendetektor-Felder
    - Cherenkov Detektoren
    - Fluoreszenzteleskope
    - Radiodetektoren
  - Observatorien
    - KASCADE und das Pierre Auger Observatorium
- Zusammenfassung

Motivation

- Benutze „herkömmliche“ Physik um Astro-physikalische Objekte zu beschreiben z.B.:
  - Evolution / Innere Struktur von Sternen
  - Dynamik von Galaxien

- Benutze Astrophysik um Hinweise auf neue Physik zu finden z.B.:
  - Helium
  - Kohlenstoff-Resonanzen
  - Neutrino Flavor
  - Dunkle Materie und -Energie
  - Neutronensterne und Schwarze Löcher

Kosmische Strahlung

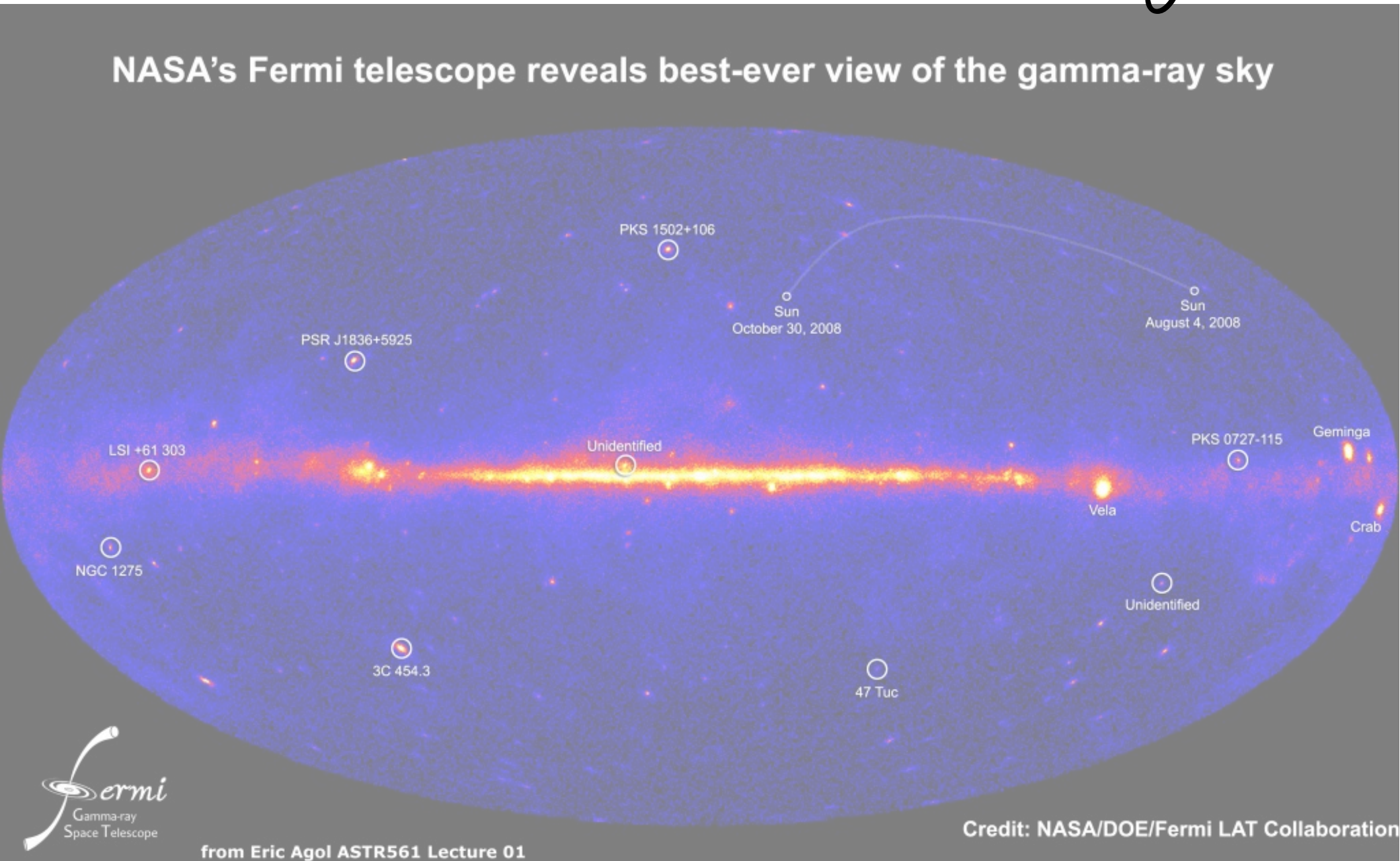

from Eric Agol ASTR561 Lecture 01

Kosmische Strahlung

- Energie: 10 eV bis 10^{21} eV
- Photonen
  - Nicht beobachtbar von 13,6 eV bis 100 eV
- Elektronen / Positronen
  - Keine Richtung für kleine Energien
- Protonen / Antiprotonen
- Atomkerne
  - Keine Antikerne schwerer als Tritium

Kosmische Strahlung

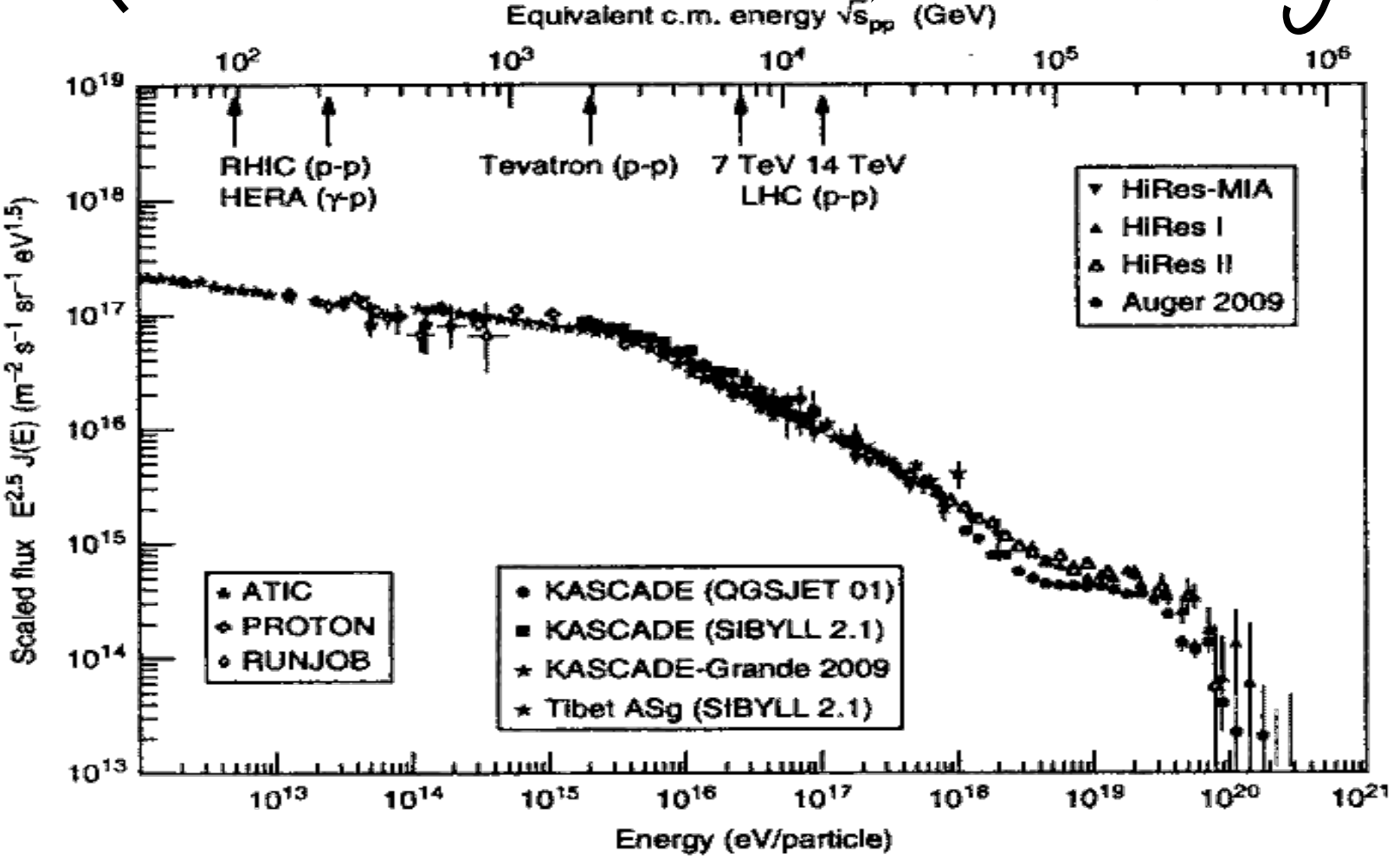

Fig. 1

All-particle flux of cosmic rays arriving at Earth, scaled by $E^{2.5}$. The equivalent center-of-mass energy of the collision with air, for protons as cosmic ray particles, is given on the upper horizontal axis. Direct measurements are shown from the balloon experiments ATIC and RUNJOB and the PROTON satellites. All high-energy data are based on indirect measurements. See Blümer et al. (2009) for refs. to the data

Chandra

Ein Röntgenspektrometer

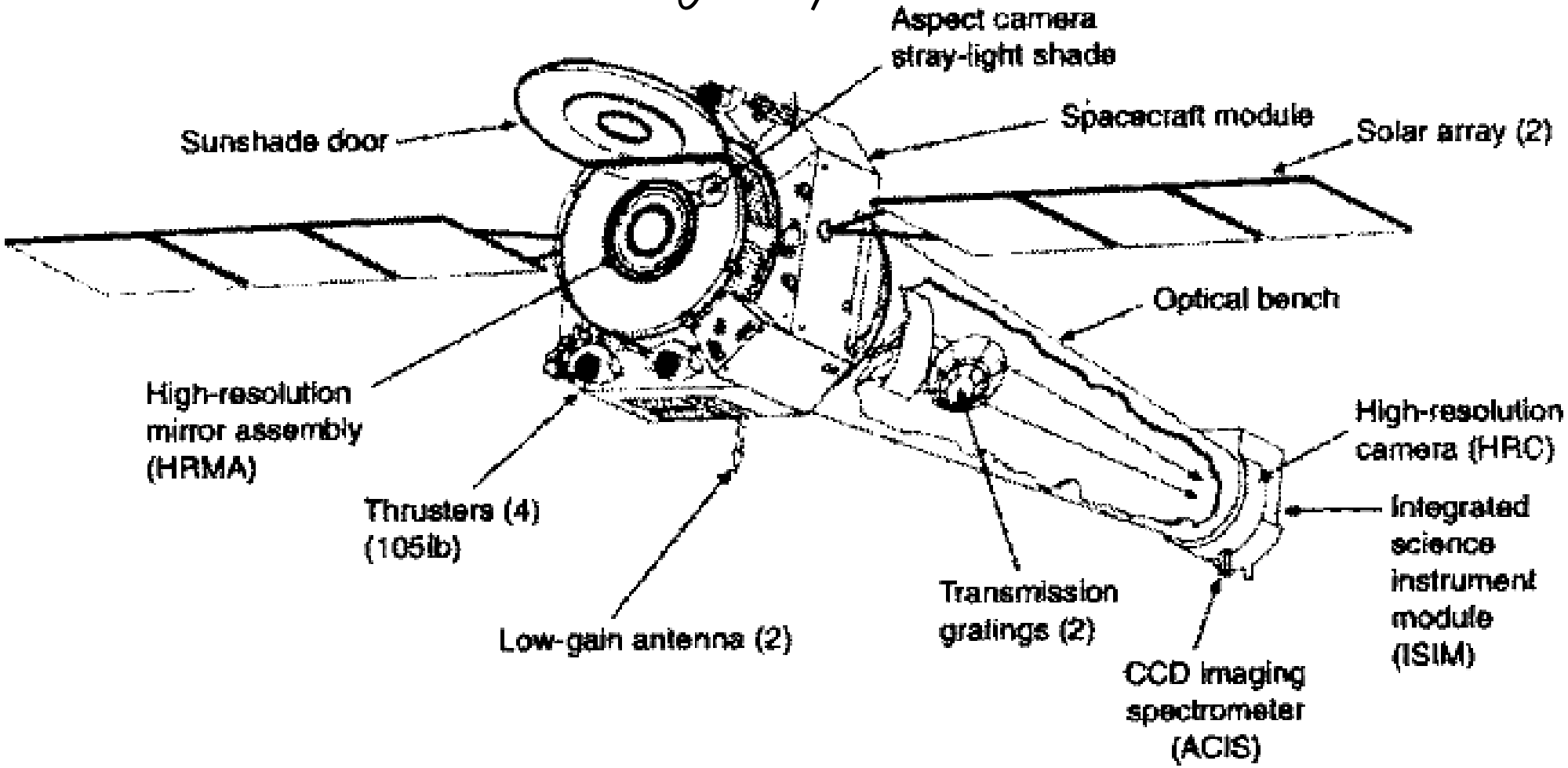

Fig. 2

Chandra spacecraft (NASA/CXC/NGST)

Chandra

Ein Röntgenspektrometer

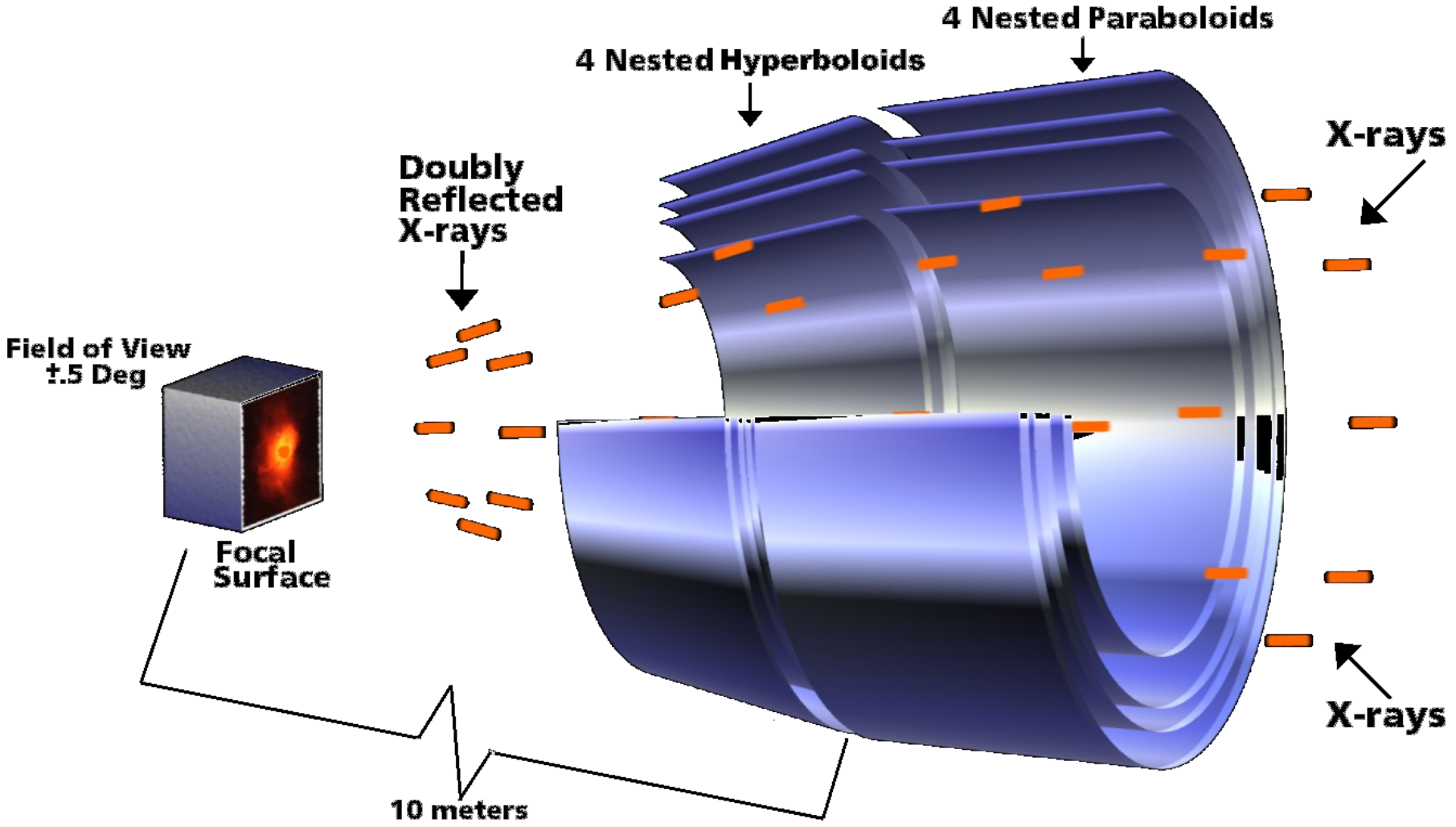

Bild: NASA/CXC/SAO

ULEIS @ ACE

- ULEIS: Ultralow-Energy Isotope Spectrometer
- ACE: Advanced Composition Explorer
- Größe: 1 m × 1,6 m
  Ohne Solarpanels
- Gewicht: 785 kg
  (incl. 189 kg Treibstoff)
- Leistung: 500 W
- Entfernung zur Erde:
  1 500 000 km

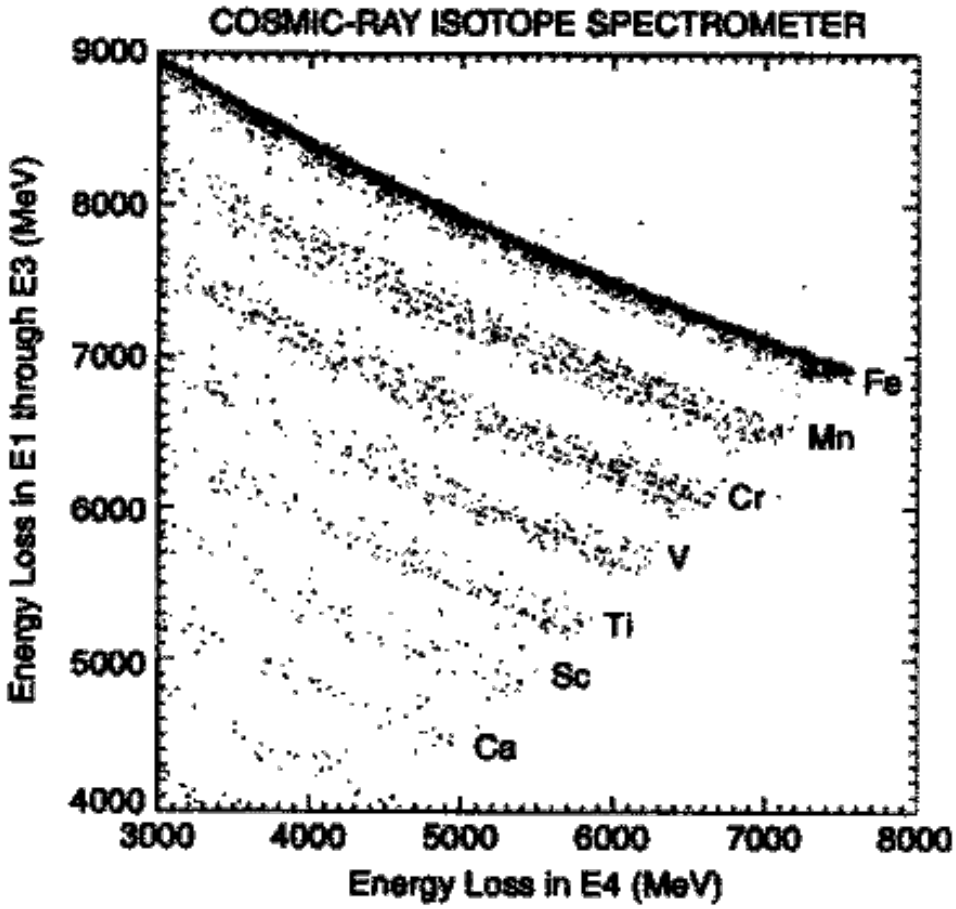

Fig. 6
dE/dx vs E technique used with ACE/CRIS (Stone et al. 1998c)

ULEIS @ ACE

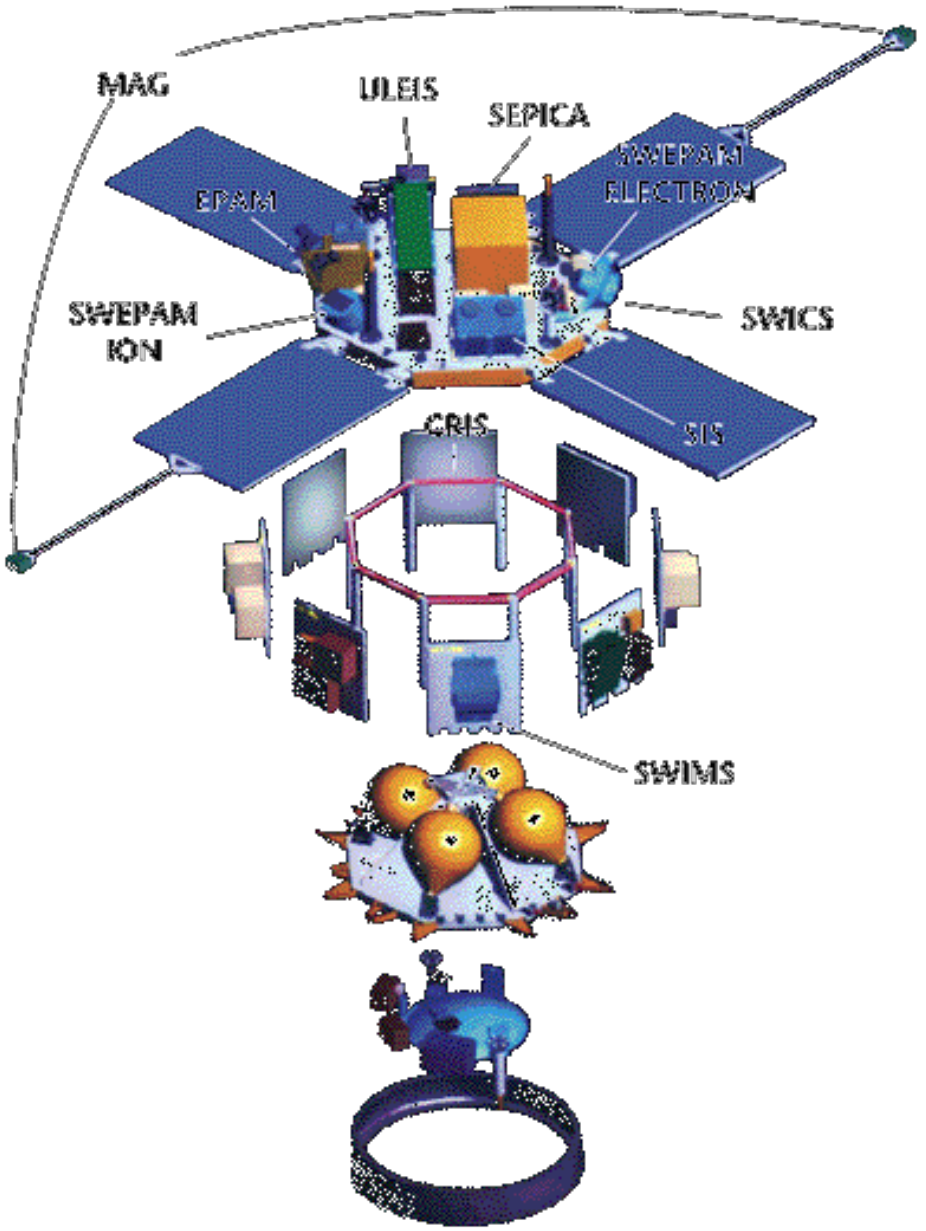

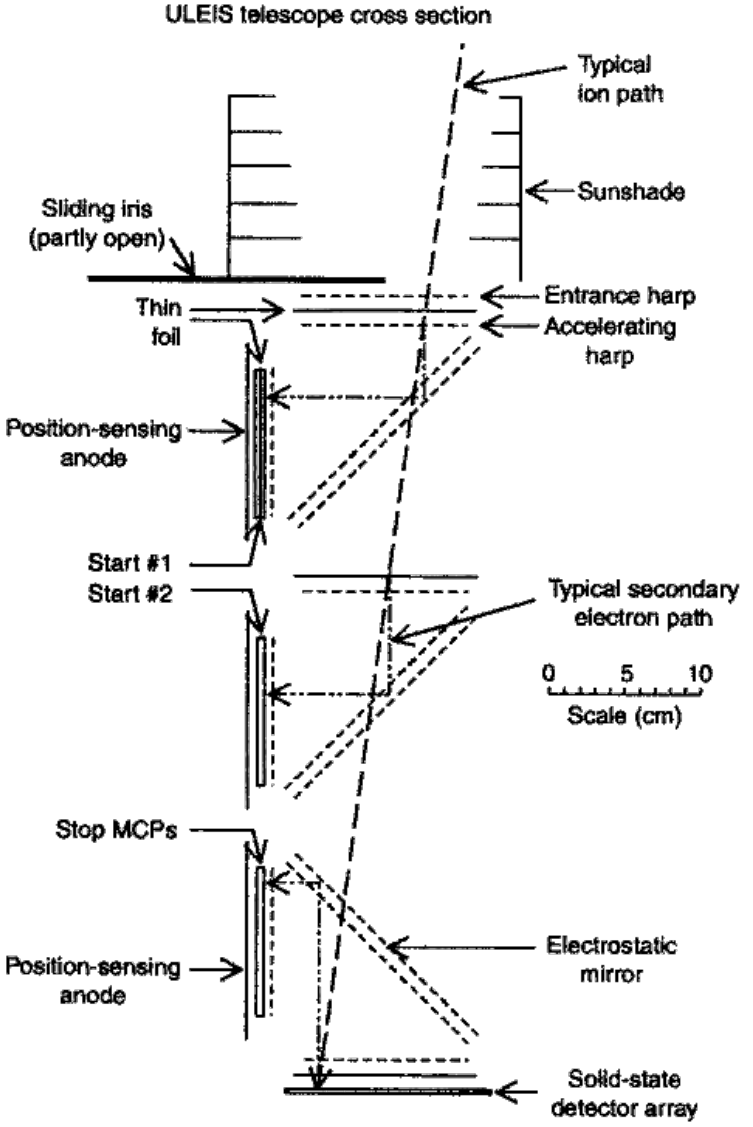

Fig. 5
Cross-sectional view of the ultralow-energy isotope spectrometer onboard ACE (Mason et al. 1998)

Bild: http://www.srl.caltech.edu/ACE/

PAMELA

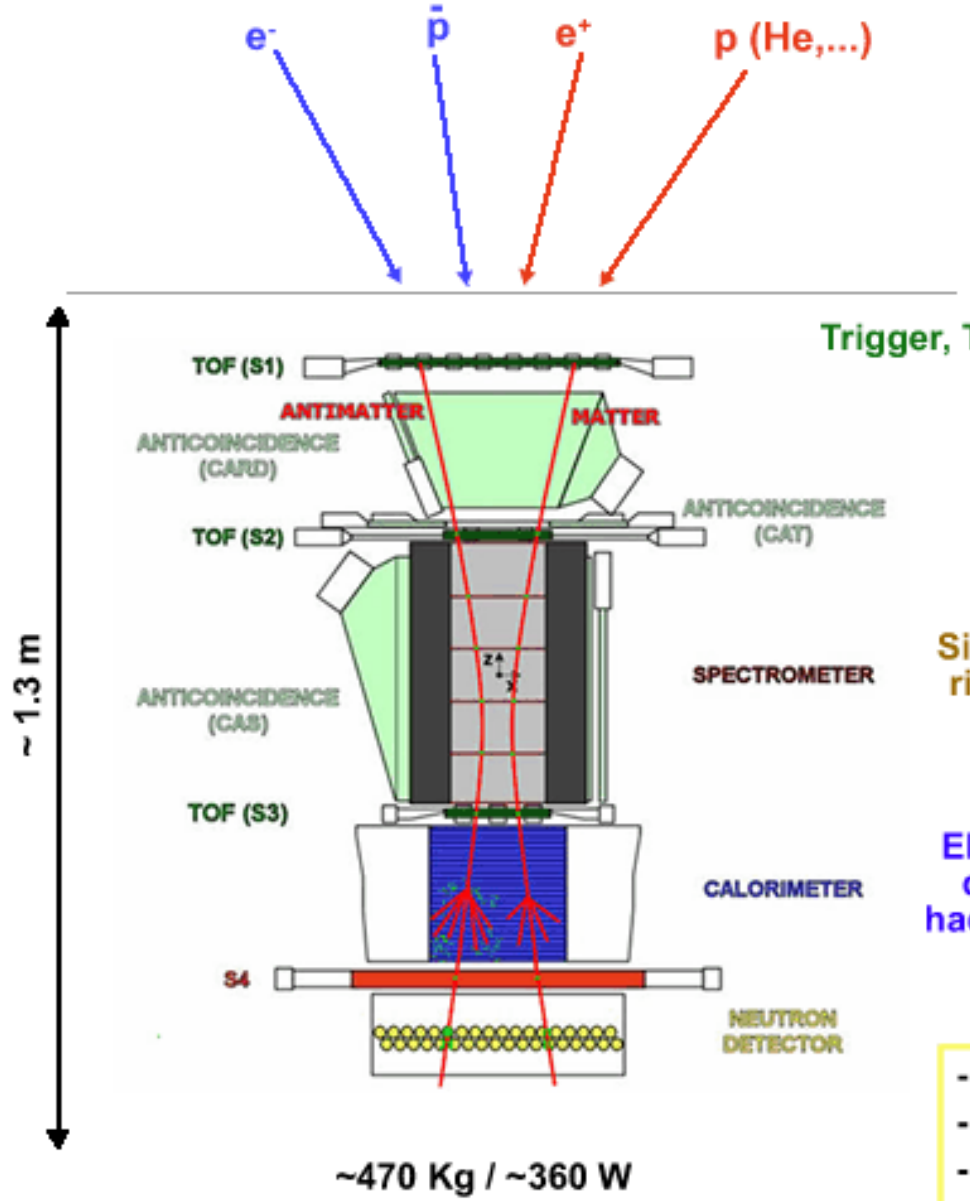

~470 Kg / ~360 W

Trigger, ToF, dE/dx

- S1, S2, S3; double layers, x-y
- plastic scintillator (8mm)
- ToF resolution ~300 ps (S1-3 ToF >3 ns)
- lepton-hadron separation < 1 GeV/c
- S1.S2.S3 (low rate) / S2.S3 (high rate)

Sign of charge, rigidity, dE/dx

- Permanent magnet, 0.43 T
- 21.5 cm^2 sr
- 6 planes double-sided silicon strip detectors (300 μm)
- 3 μm resolution in bending view → MDR ~800 GV (6 plane) ~500 GV (5 plane)

Electron energy, dE/dx, lepton-hadron separation

- 44 Si-x / W / Si-y planes (380)
- 16.3 X0 / 0.6 L
- dE/E ~5.5 % (10 - 300 GeV)
- Self trigger > 300 GeV / 600 cm^2 sr

- 36 ^{3}He counters
- ^{3}He(n,p)T; E_p = 780 keV
- 1 cm thick poly + Cd moderator
- 200 μs collection

Bild: http://pamela.roma2.infn.it

PAMELA

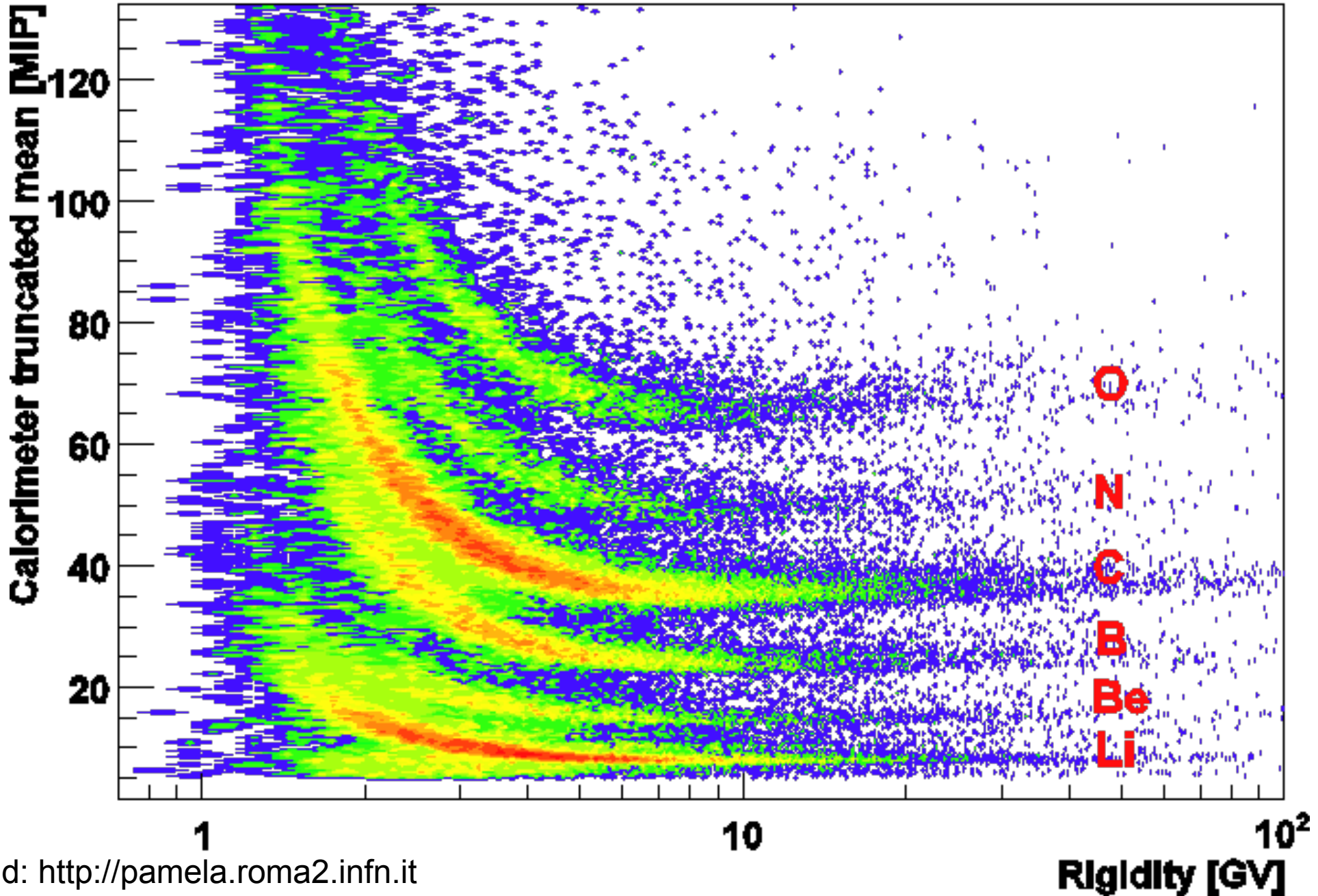

Bild: http://pamela.roma2.infn.it

Teilchenschauer

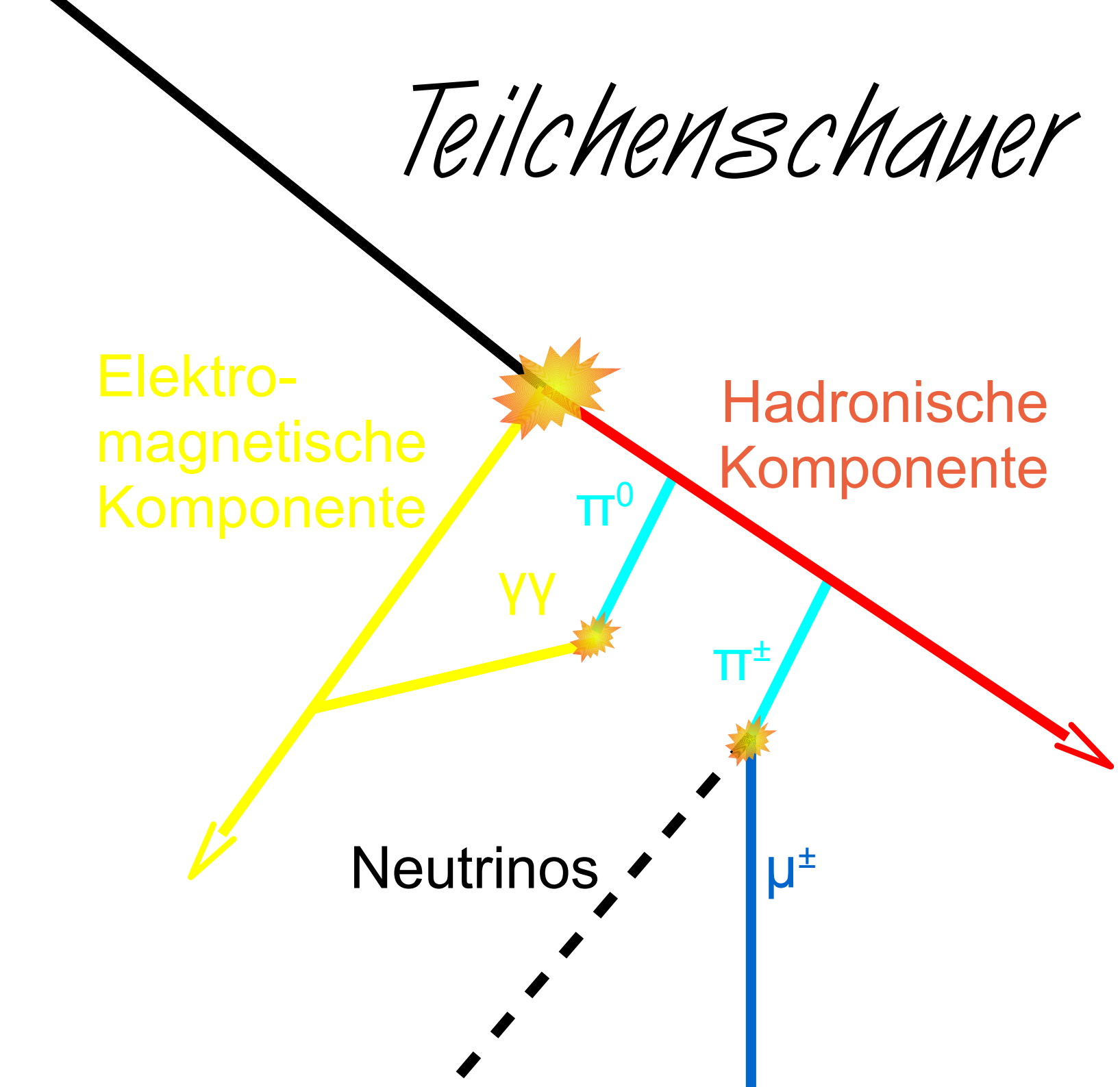

Teilchenschauer

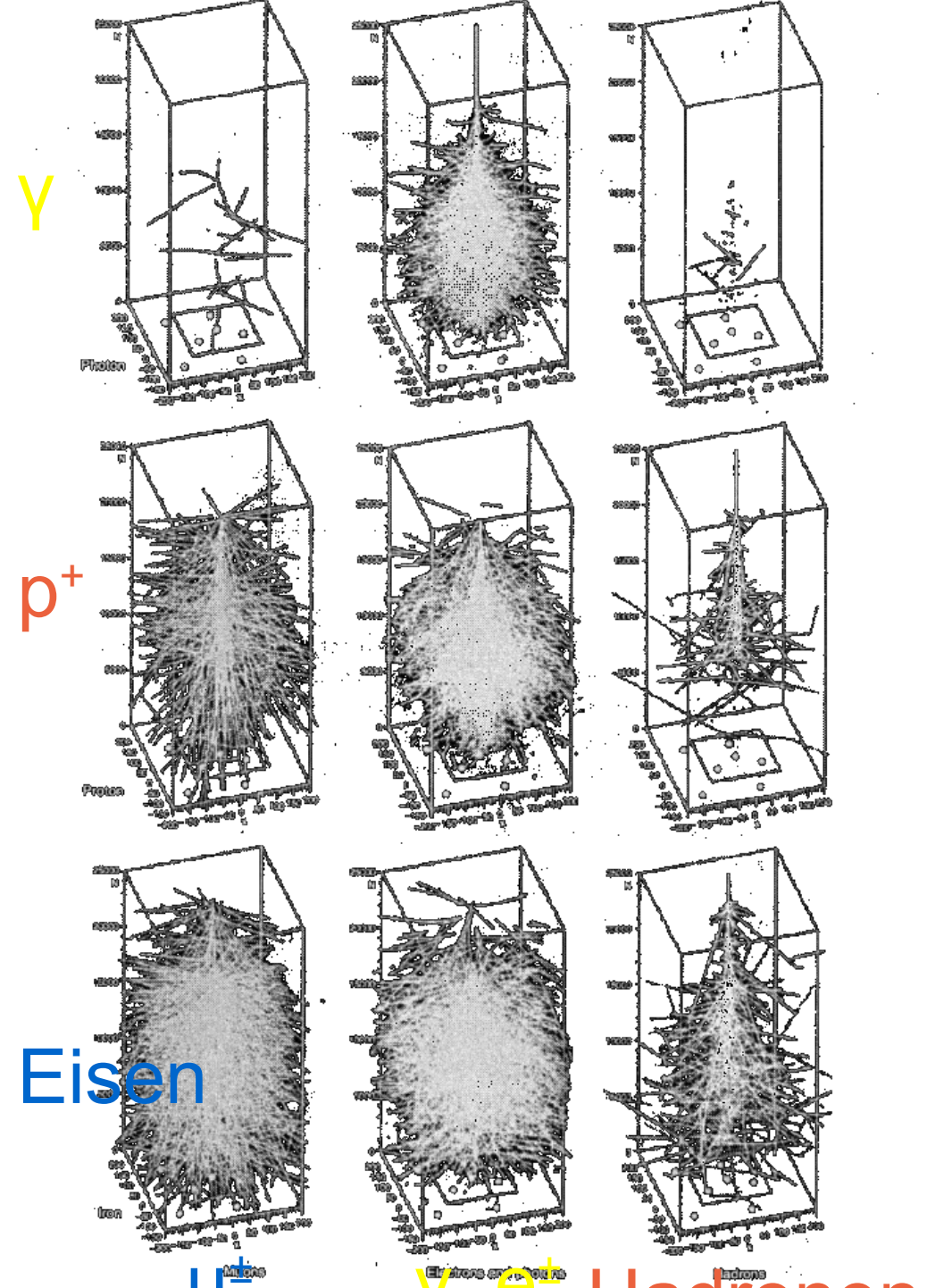

Fig. 2
Tracks of secondary particles of air showers induced by a photon, proton, and iron nucleus. The height of the graphs corresponds 25 km, and the width is 400 m. The simulations were done with CORSIKA.

Querschnitt eines Schauers

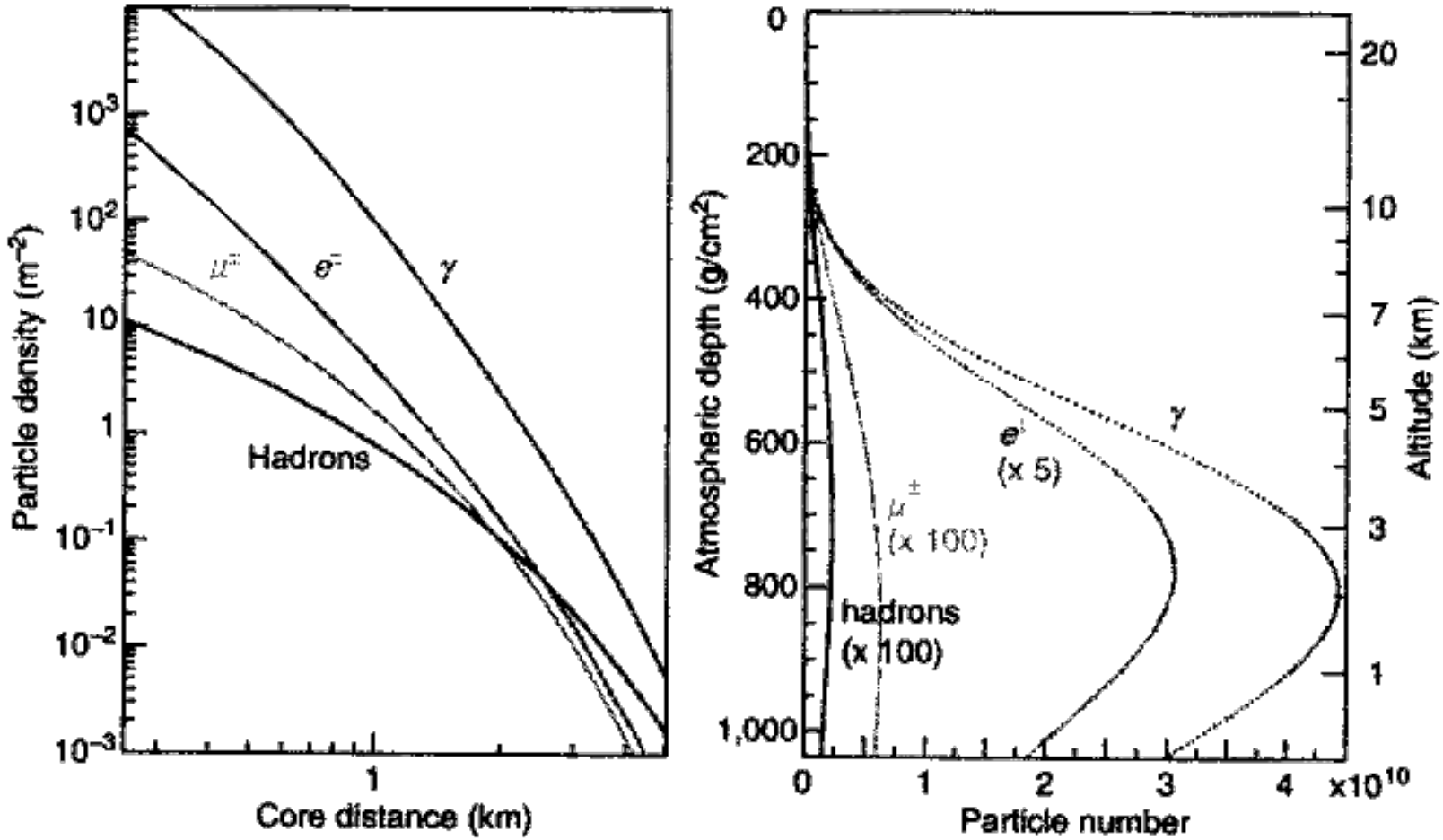

Fig. 3

Lateral and longitudinal shower profiles for vertical, proton-initiated showers of 10^{19} eV simulated with CORSIKA. The lateral distribution of the particles at ground is calculated for 870 g/cm^2, the depth of the Auger Observatory. The energy thresholds of the simulation were 0.25 MeV for γ, $e^{\pm}$ and 0.1 GeV for muons and hadrons. From Engel et al. (2011)

Teilchendetektor-Felder

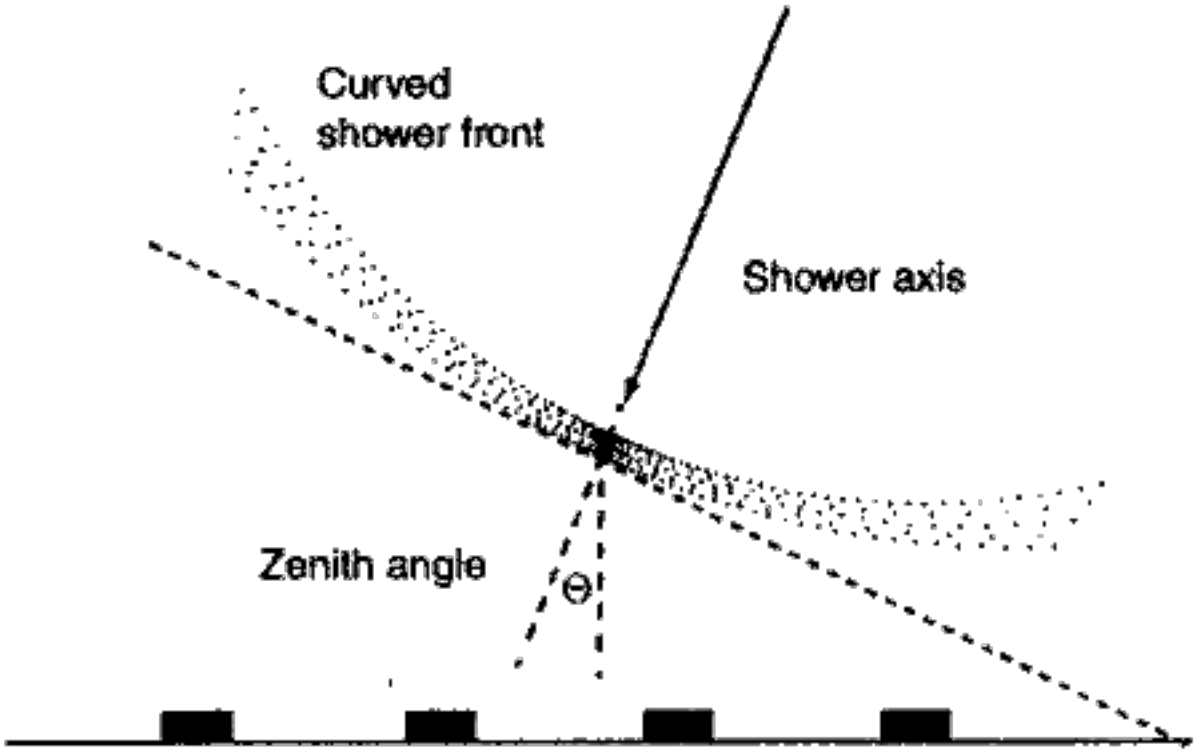

Fig. 4

Detection principle and geometry reconstruction of air showers with surface detector arrays

- Typ. Abstand: 13 m (KASCADE) bis 1000 m (Teloscope Array, Auger Observatorium)
- Typ. Winkelauflösung: 0,5° bis 2°

Primär-Teilchefidentifikation

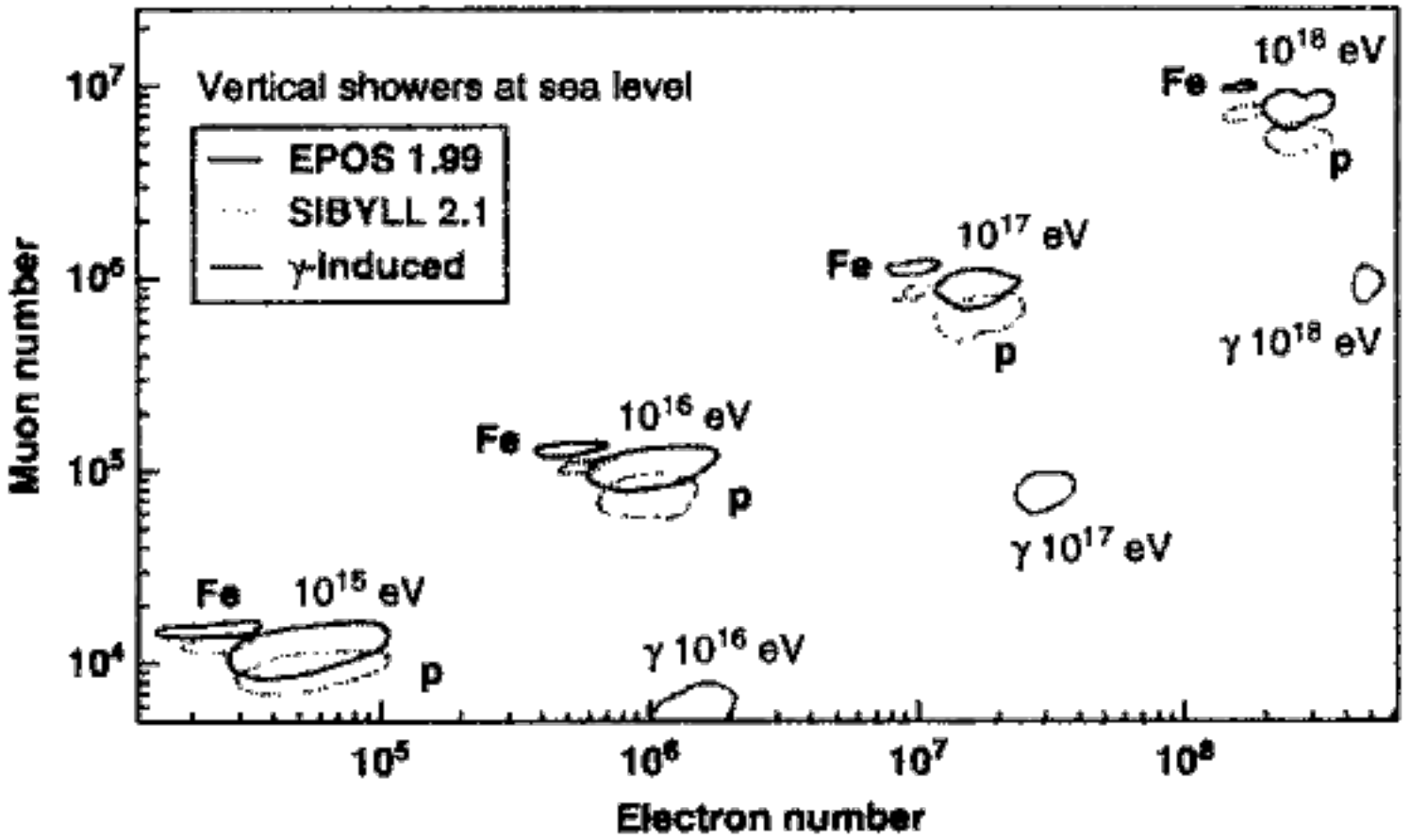

Fig. 6

Predicted correlation between the number of muons and electrons of vertical showers at sea level. The simulations were done with CORSIKA using the same cutoff energies for the secondary particles as in *Fig. 3*. The curves encircle approximately the one-sigma range of the fluctuations. From Engel et al. (2011)

Cherenkov-Strahlung

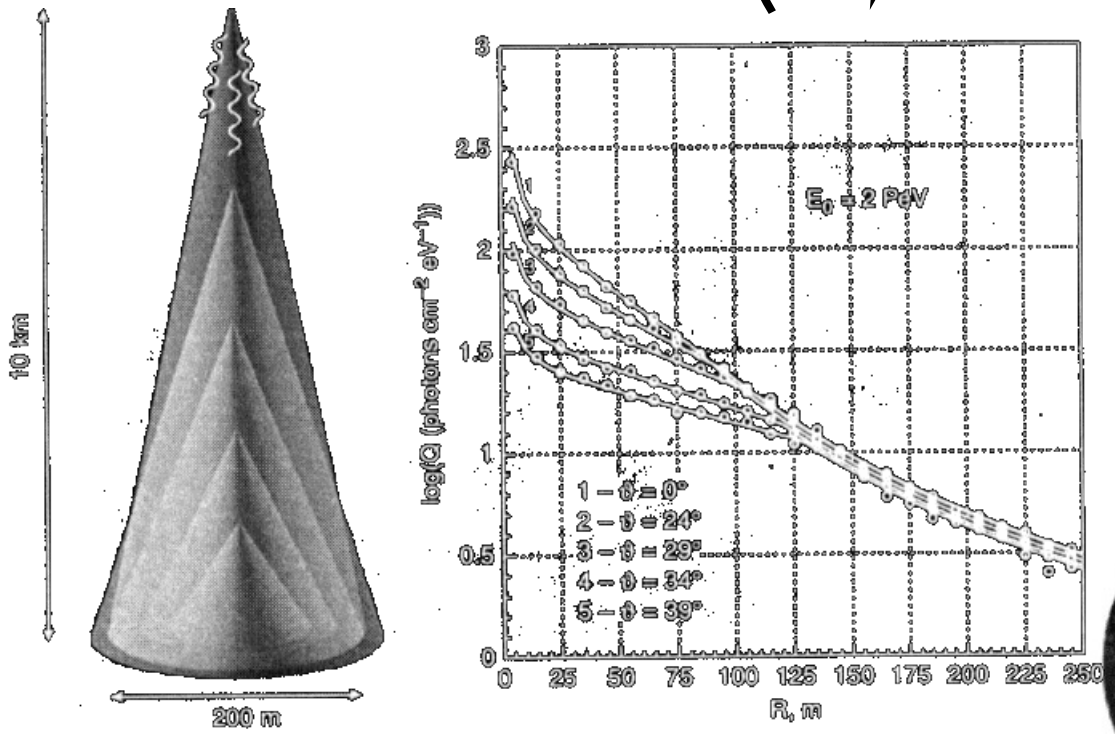

Fig. 7

Left: Illustration of the relation between production height and Cherenkov opening angle for producing the observed Cherenkov light distribution at ground. *Right*: Simulated lateral distributions of Cherenkov light produced by proton-induced showers of different zenith angle (Korosteleva et al. 2003). The simulations were done for a height of 2,000 m above sea level

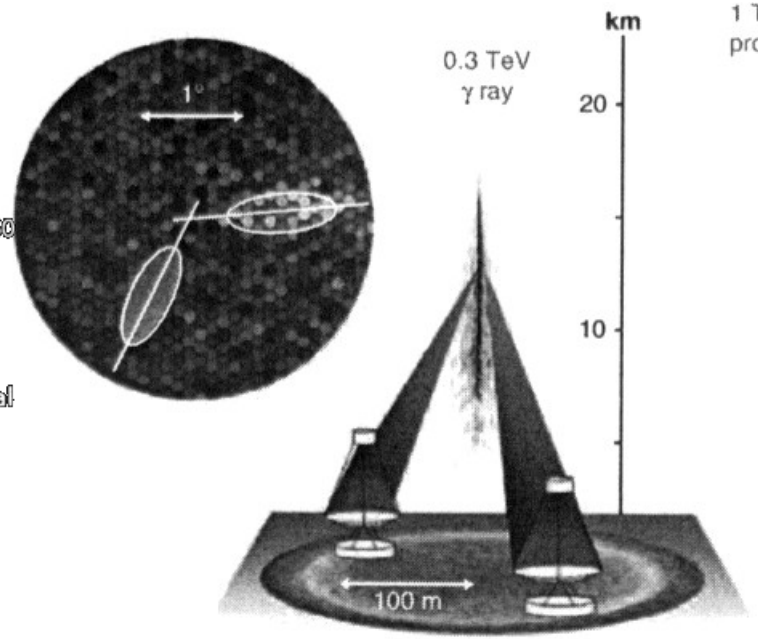

Fig. 8

Illustration of the stereo-detection principle of imaging atmospheric Cherenkov telescopes (Hinton and Hofmann 2009). The superimposed camera images are shown on the *left-hand side*. The intersection of the shower axes in this combined image corresponds to the arrival direction of the shower

Fluoreszenz-Strahlung

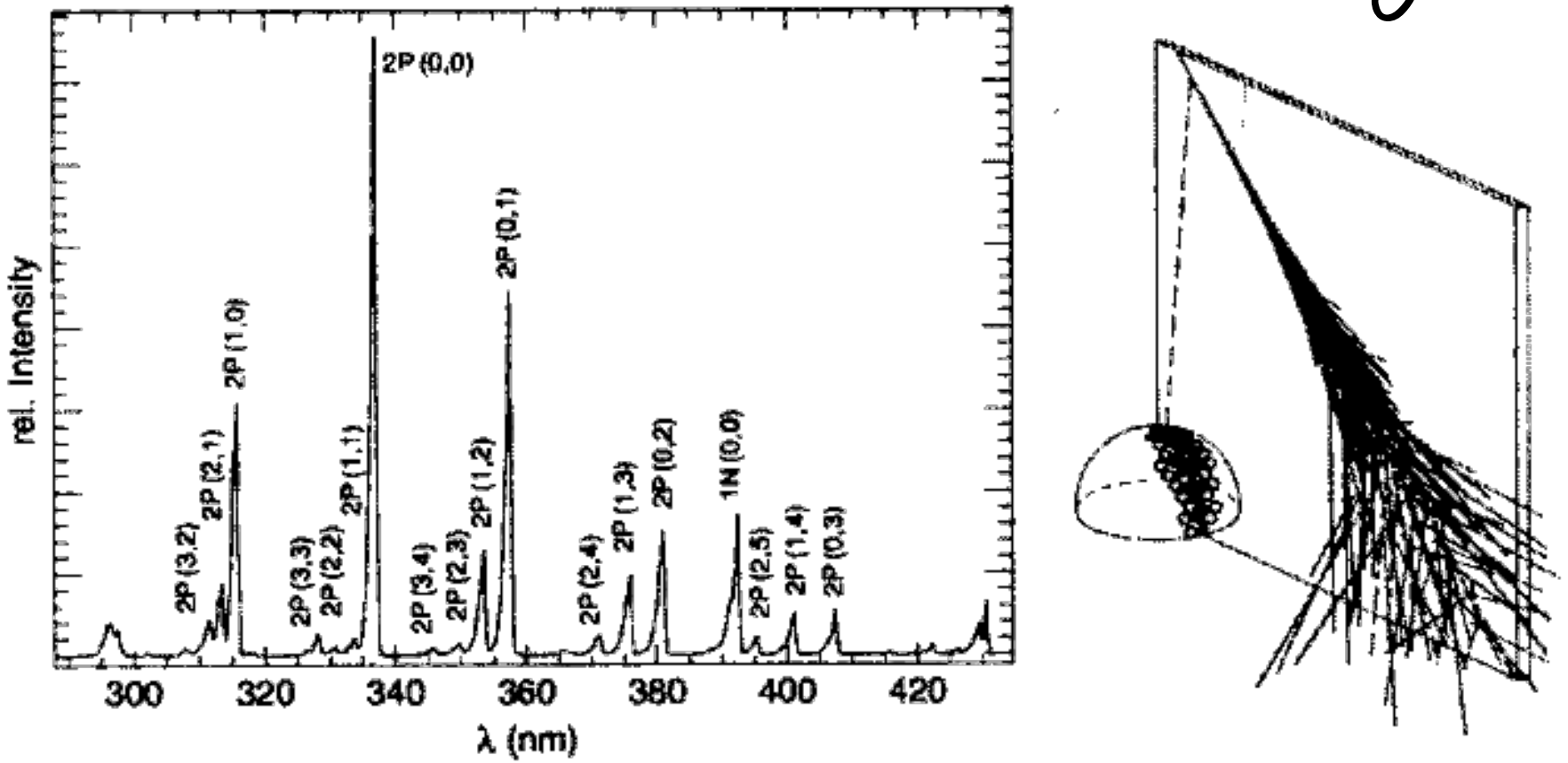

Fig. 9

***Left*: Fluorescence light spectrum of air at 20 °C and 800 hPa (Arciprete et al. 2006). The bands are labeled with the electronic transition type (2P or 1N) and the change of the vibration quantum number. *Right*: Illustration of the detection principle of fluorescence telescopes. The arrival angle of the shower can be measured with high precision in the shower–detector plane**

Radio Signalmessung

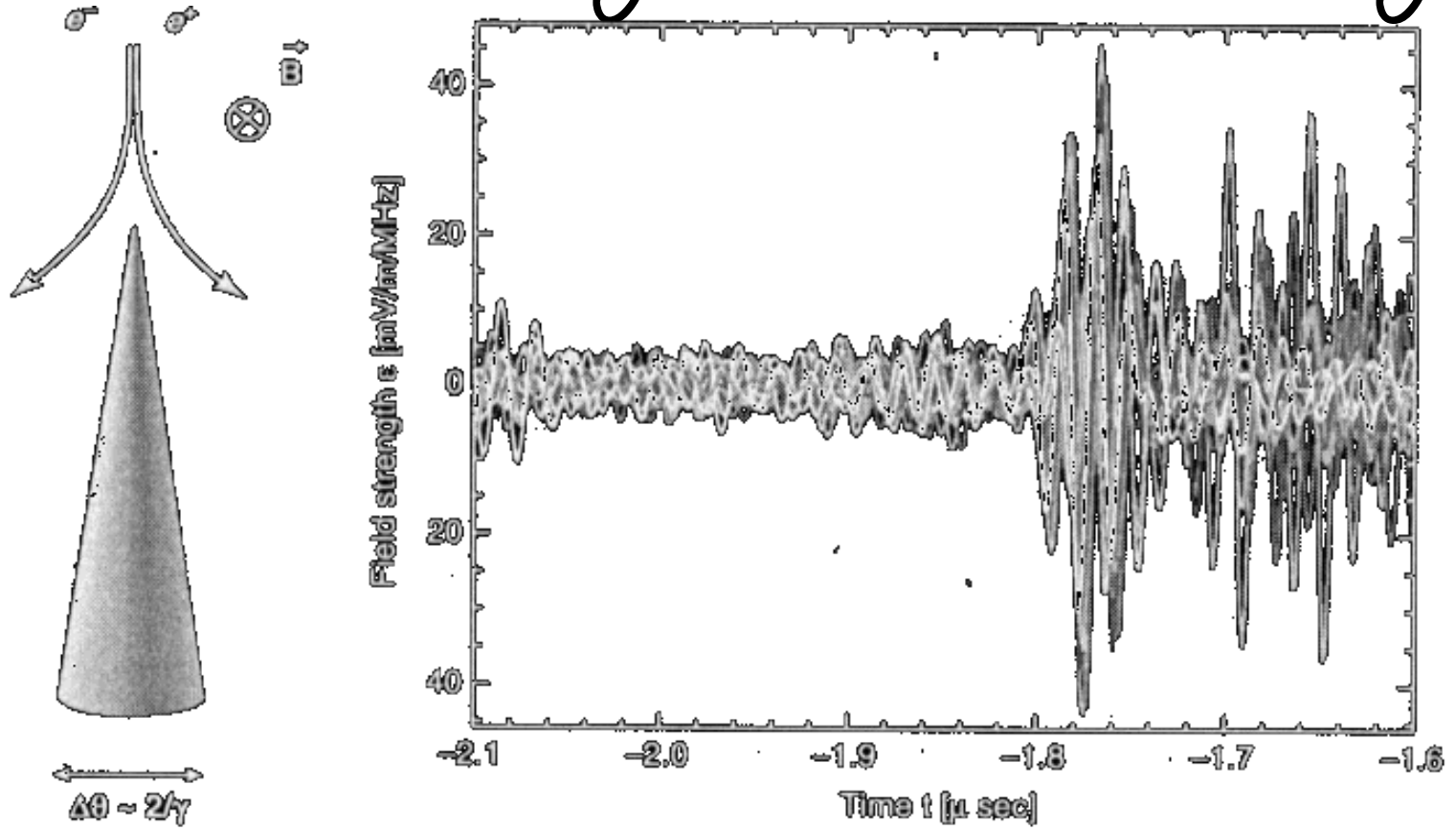

Fig. 11

Left: Illustration of synchrotron radiation of an e^+e^- pair in the geomagnetic field. The radiation is beamed and the opening angle of the cone is about $1/\gamma$, with γ being the Lorentz factor. *Right*: Radio pulse measured with LOPES in the frequency range 40–80 MHz (Apel et al. 2010). Different lines show the signal from different radio antennas. The incoherent signal after the radio pulse (starting at −1.7 μs) stems from the particle detectors in the KASCADE array

KASCADE

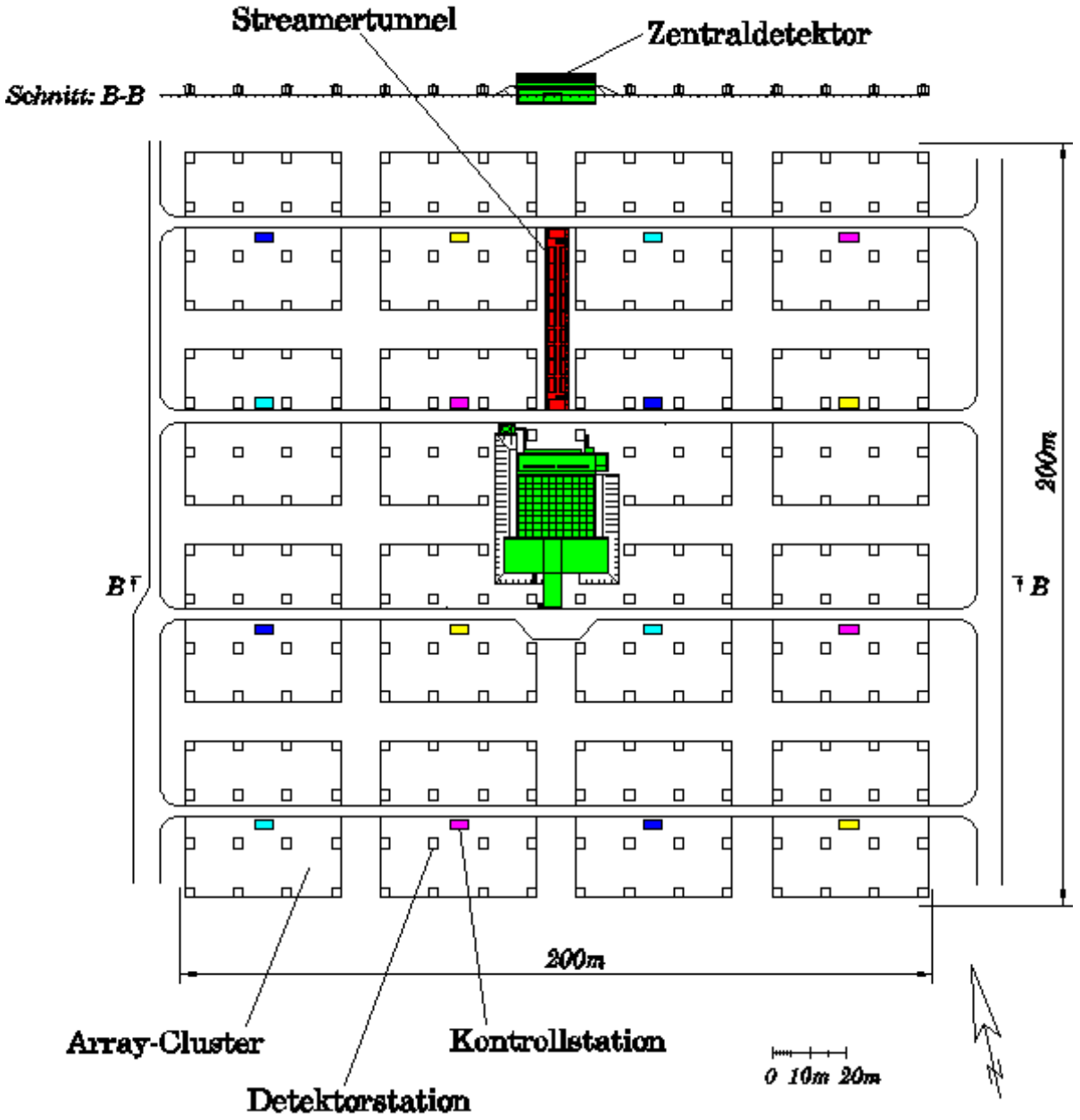

KArlsruhe **S**hower
Core and **A**rray
DEtector

Bild: http://www-ik.fzk.de

KASCADE

KArlsruhe **S**hower **C**ore and **A**rray **DE**tector

Bild: http://www-ik.fzk.de

KASCADE

KArlsruhe **S**hower
Core and **A**rray
DEtector

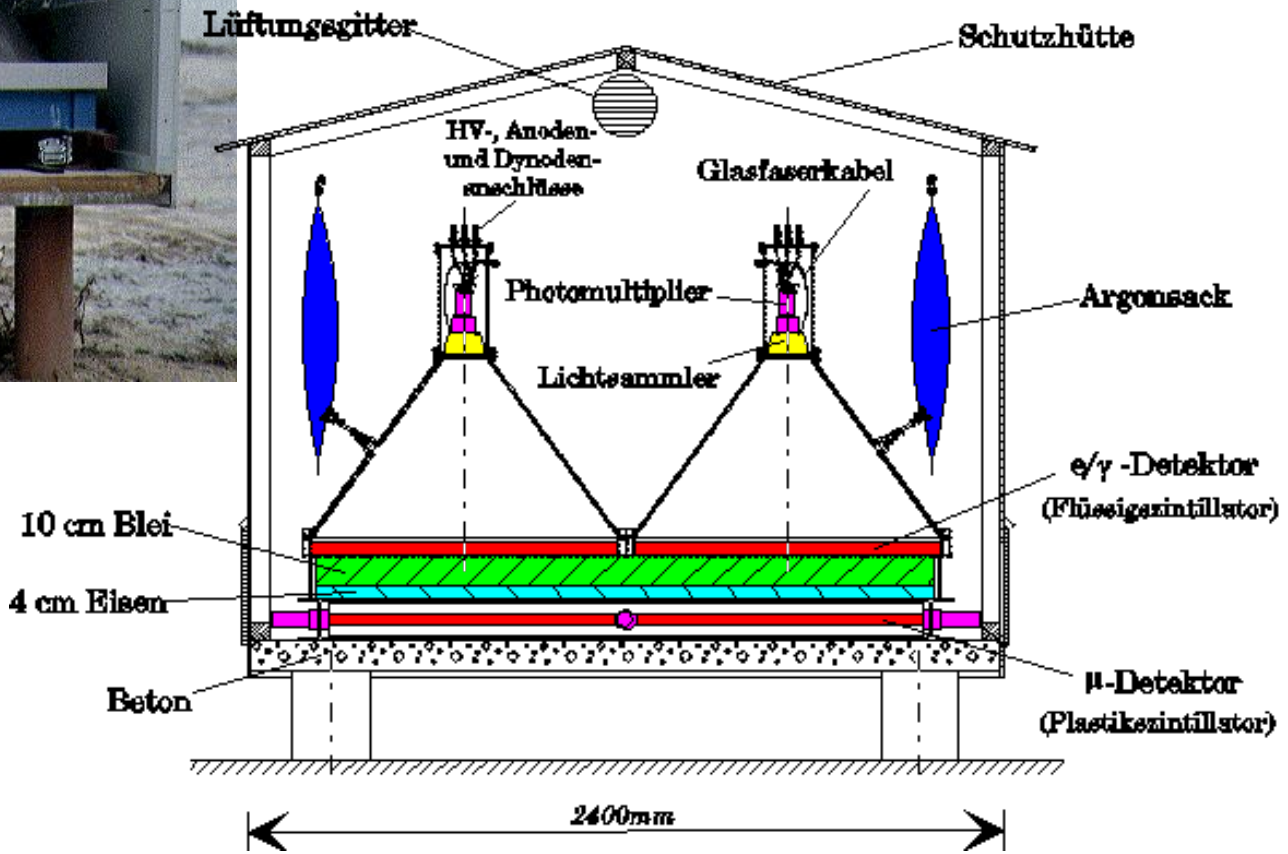

Bilder: http://www-ik.fzk.de

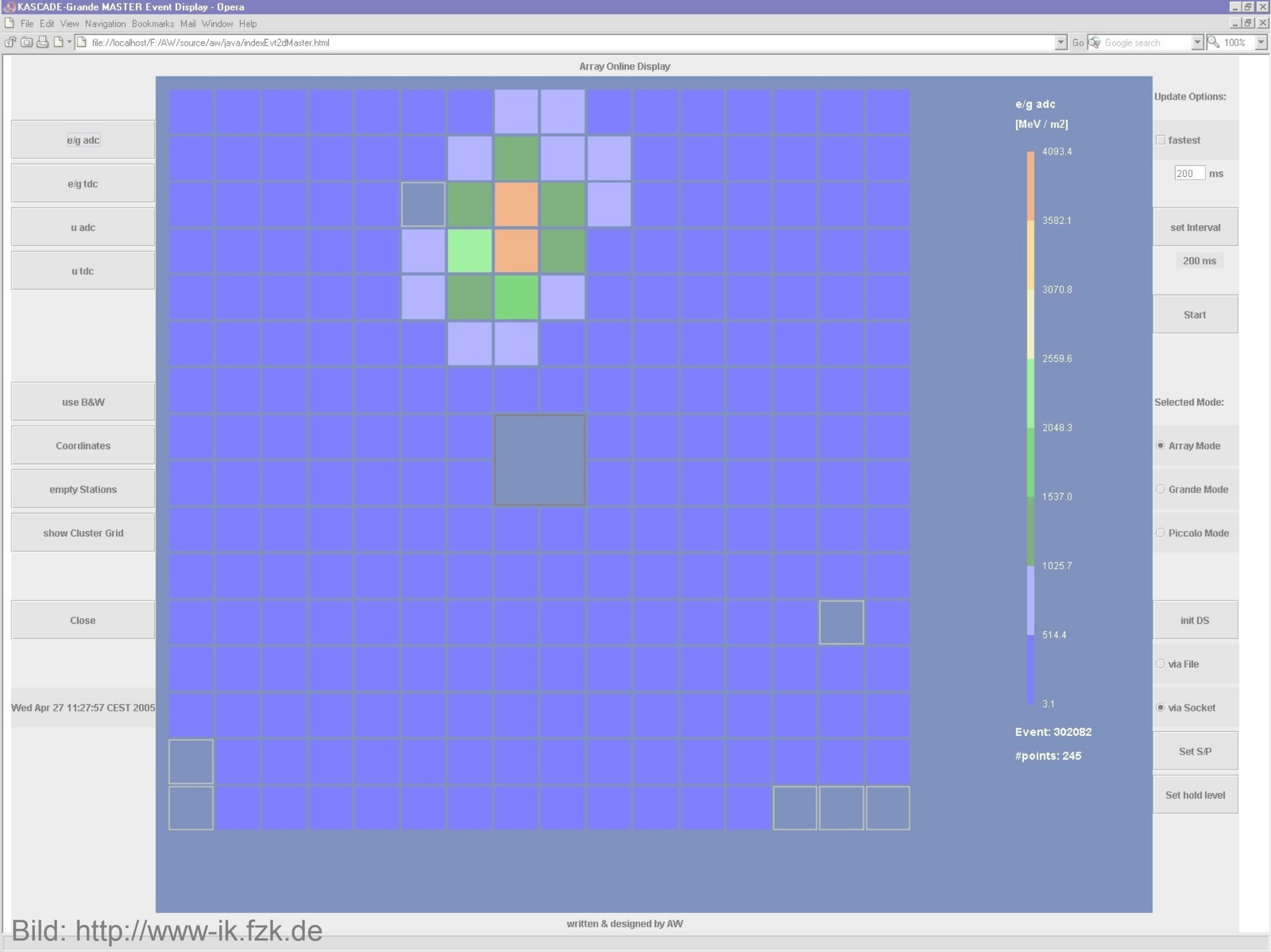

Bild: http://www-ik.fzk.de

Pierre Auger Observatorium

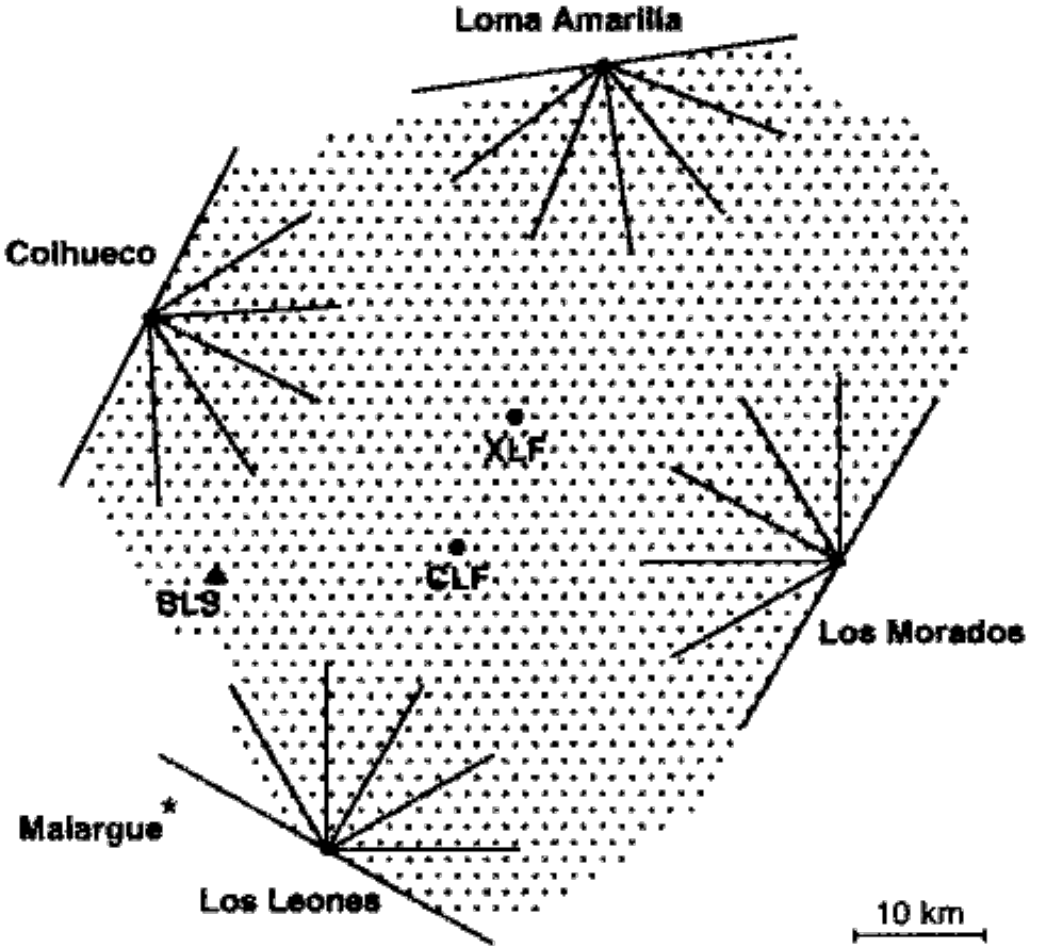

Fig. 16

Layout of the Auger Observatory in Argentina. Shown are the locations of the 1,600 surface detector stations. The field of view of the fluorescence telescopes is indicated by lines. Also marked are the locations of the two laser facilities in the array (CLF and XLF) and the balloon launching station (BLS)

Pierre Auger Observatorium

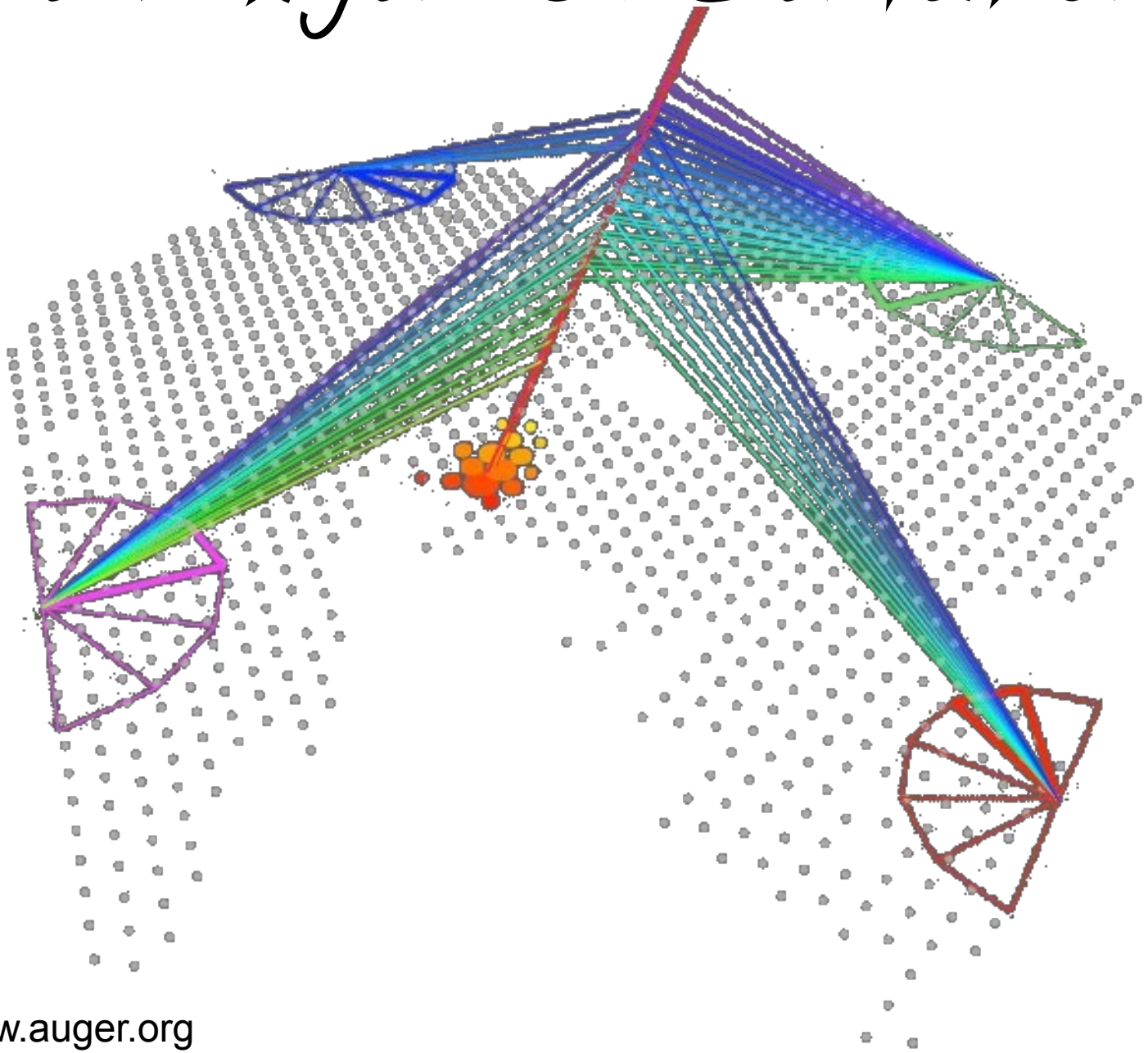

Bild: http://www.auger.org

Bild: http://www.auger.org

Zusammenfassung

- Die Beobachtung von kosmischer Strahlung ist von hoher Bedeutung für das Verständnis des Kosmos.
- Direkte Messungen sind das Mittel der Wahl für kleine Energien, wo die Teilchenflüsse hoch sind.
- Für größere Energien verwendet man die Atmosphäre als Detektor.
  => Gutes Verständnis der atmosphärischen Bedingungen am Messort benötigt
- Für atmosphärische Schauer gibt es keine Theorie sondern nur Simulationen.
  => Große systematische Unsicherheiten

Quellen

[1] C. Grupen, I. Buvat (eds.),
Handbook of Particle Detection and Imaging,
Springer-Verlag Berlin Heidelberg 2012,
Kapitel 23 & 24

Alle Bilder stammen aus diesem Buch, soweit nichts anderes angegeben

[2] Eric Agol, University of Seattle,
Script zur Vorlesung „*High Energy Astrophysics*“

Homepages der Projekte:
[3] http://www.srl.caltech.edu/ACE
[4] http://chandra.harvard.edu
[5] http://pamela.roma2.infn.it
[6] http://www-ik.fzk.de
[7] http://www.auger.org

Fragen

- ...